Track Occupancy Detection Using Ratio of Open-Circuit Impedance to Short-Circuit Impedance

Lubomir IVANEK[1], *Petr ORSAG*[1], *Vladimir MOSTYN*[2], *Karel SCHEE*[3]

[1]Department of Electrical Engineering, Faculty of Electrical Engineering and Computer Science, VSB–Technical University of Ostrava, 17. listopadu 15, 708 00 Ostrava, Czech Republic
[2]Department of Robotics, Faculty of Mechanical Engineering, VSB–Technical University of Ostrava, 17. listopadu 15, 708 00 Ostrava, Czech Republic
[3]Prvni signalni a.s., Bohuminska 368/172, 712 00 Ostrava, Czech Republic

lubomir.ivanek@vsb.cz, petr.orsag@vsb.cz, vladimir.mostyn@vsb.cz, schee@1sig.cz

DOI: 10.15598/aeee.v16i2.2662

Abstract. *This paper deals with the change of the ratio of the open circuit impedance to short-circuit impedance of the electric traction depending on the distance of the traction vehicle from the beginning of the section. This ratio is calculated in order to estimate the traction vehicle speed and the distance at which the track occupancy can be indicated. Therefore, the impedance moduli and the impedance phases of the open track circuit and the impedance of the occupied track (short-circuit impedance) is compared at different short-circuit distances. The impedances ratio varies with changing weather conditions. It is different in dry weather than in the rain. Therefore, in practical use, the track occupancy indicator must always be updated and the ratio must always be recalculated for the new situation. In this paper, the impedances ratio is calculated for specific parameters measured in the section of the track in Orlova. The distance between a reference point (place of short circuit rails) from a measuring point is for the impedance module ratio of F =10 about 218 m.*

Keywords

Impedance, occupied track, rail, traction, two-port.

1. Introduction

This paper is aimed at estimating how the parameter $\underline{F}$ of railway traction is changed depending on the length of the occupied section. $\underline{F}$ is the ratio of the input impedance of the unoccupied track circuit section to the input impedance of the occupied track parts of the same traction section. Input impedance measurements can be used for the occupancy detection of the examined section if ratio $\underline{F}$ is large enough. This paper uses data measured at the traction in Orlova as a model example. Thus, the dependence of $\underline{F}(x)$ on the variable x was calculated based on the results of the measurement of the insulated section of the traction in the Orlova.

The ratio $\underline{F}(x)$ of the open-circuit input impedance $\underline{Z}_0$ to the short-circuit input impedance $\underline{Z}_S$ on the length x of the examined section was calculated. The impedance of open-circuit $\underline{Z}_0$ is defined as the impedance of the open rail section of a length l_0. From the value $x = l_0$ with increasing distance x (i.e. distance from the measuring point), the open-circuit impedance is no longer changing. We divided this constant open-circuit impedance value $\underline{Z}_0$ by the input impedance of the short-circuit $\underline{Z}_S(x)$ for the different lengths x of the sections to obtain the desired dependence $\underline{F}(x)$ as a function of the variable x.

The tractions are a highly variable system from an electrical point of view. This concerns the differences in the track layout on different tracks and at different locations, as well as the dependence of track parameters on weather conditions. The space between the rails is often dirty, the distance of the rails from earth is different. Frequently, the rails are in direct contact with gravel, which fills the space between them. The gravel may be streaked with vegetation that touches the rails. When evaluating the occupancy of the section, electrical parameters of the track change with the weather conditions and the time variability of the operating conditions must also be taken into account. Therefore, determining the parameters of rail traction is a very complex task. The time-varying conditions for alternating currents (injected into rails for track circuits protection) in practical applications require the regular calibration of devices, the function of which is based on the evaluation of the traction electrical parameters. In this model example we do not take in the account the impedance between the wheels of the traction vehicle which could increase the transverse or longitudinal impedance of the section of railway line.

The occupancy of railroad tracks by the train wheels and axles should be detected, for example, near the railway crossing. Therefore, security devices must recognize if the section is occupied. It is often also required to determine the speed of an approaching vehicle. The occupied section appears to us as a short-circuit in the place where the traction vehicle is located (the low impedance of rails short circuit through the wheels and axles of the traction vehicle is neglected).

A category of the "Early Detection" system is appropriate [1] for the detection of the position and speed of a train before railway crossing. These devices are mounted at the crossing point only and do not use any remote sensors. There are multiple principles in this category - for example, radar systems using Doppler's principle of speed measurement, Time-Domain Reflectometry [2] - transmitting impulse to track circuit and measuring transmission delay after its reflection, and even acoustic systems based on the horn sound analysis. A very good principle for detecting the train's position and speed, also included under the "Early Detection" category, is to measure the waveform of the impedance of the track circuit, which is shorted by the front and other axles of the incoming train. This principle is already in use, but its safe use is greatly hampered by the high level of interference of the measuring signals caused by electric traction drives of trains, by the transmission of signaling by means of track circuits and other sources of electrical interference. However, with the development of fast Digital Signal Processors (DSPs), it is possible to construct a measuring device resistant to this interference and to accurately analyze the short-circuit impedance of the track circuit.

The sensitivity of the methods comparing the changes in the impedance to the occupied and unoccupied track can be judged by the waveform of the impedances ratio $\underline{F}(x)$ measured on the open track $\underline{Z}_0$ and the impedance on the short-circuited track $\underline{Z}_S$. According to this ratio, we can deduce the place of the short-circuit and ultimately the speed of the approaching vehicle. Obviously, at a certain critical distance l_k, the ratio is so small that we will not register the arriving vehicle. The dependence of the ratio $\underline{F}(x)$ on the distances x from the measuring point can be described by the analytical function and implemented in the DITO (Device for Indicating of the Track Occupancy) device for detecting track occupancy. Both the modulus ratio $\underline{F}(x)$ and its phase can be evaluated. The second reason for detection of the open-circuit to short-circuit impedance ratio $\underline{F}(x)$ are frequent time changes of both impedances, caused in particular by changes in the conductivity of the subsoil and track sleepers [3]. While the open-circuit impedance fluctuates greatly with the conductivity of the subsoil, the short circuit impedance varies relatively little. However, it is possible to create a calibration curve for the simulation of the position and speed of the vehicle on the track circuit due to changes in the module and phase of the impedance ratio $\underline{F}(x)$. Calibration is performed on the basis of the measurement of an unoccupied section, i.e., when there is no vehicle on the track.

We used the parameter values from Tab. 1 for all the calculations in this paper based on the impedances of the traction circuits measured on the track in Orlova [3]. In the calculations, we replaced the measured section using a Π two-port network. From the impedance of open-circuit $\underline{Z}_0$ and impedance of short-circuit $\underline{Z}_S$ (measured on the isolated section of the railway line), the transmission matrix cascading coefficients Eq. (1) and the traction parameters were first calculated.

$$\underline{\mathbf{A}} = \begin{bmatrix} \sqrt{\dfrac{\underline{Z}_0}{\underline{Z}_0 - \underline{Z}_S}} & \underline{Z}_S\sqrt{\dfrac{\underline{Z}_0}{\underline{Z}_0 - \underline{Z}_S}} \\ \sqrt{\dfrac{1}{\underline{Z}_0(\underline{Z}_0 - \underline{Z}_S)}} & \sqrt{\dfrac{\underline{Z}_0}{\underline{Z}_0 - \underline{Z}_S}} \end{bmatrix}. \tag{1}$$

Tab. 1: Open-circuit and short-circuit impedance.

Impedance $\underline{Z}_0$ open-circuit			Impedance $\underline{Z}_S$ short-circuit		
f (Hz)	$\underline{Z}_0$ (Ω)	f_0 (°)	f (Hz)	$\underline{Z}_S$ (Ω)	f_S (°)
74.76	13.25	−5.7	75.86	0.85	47.6

Per-unit-length parameters of the Π element [3] are calculated from the elements of the cascade coefficient matrix on the basis of Eq. (2) and Eq. (3) and are presented in Tab. 2. Here, for comparison, the measurements at the frequency of 275 Hz are also given.

$$\underline{Z} = \underline{A}_{12} = R + j\omega L, \tag{2}$$

$$\underline{Y} = \frac{\underline{A}_{11} - 1}{\underline{A}_{12}} = G + j\omega C. \tag{3}$$

Tab. 2: Per-unit-length parameters of Π element.

f (Hz)	R ($\Omega\cdot$km^{-1})	G ($S\cdot$km^{-1})	L ($H\cdot$km^{-1})	C ($F\cdot$km^{-1})
75	1.05e+00	1.40e-01	2.61e-03	3.68e-05
275	1.56e+00	1.51e-01	2.06e-03	6.46e-06

The parameters of different types of tracks vary considerably, as can be seen in the literature [3], [4], [5], [6], [7], [8] and [9]. We further used the parameters from Tab. 2 to create a sample model case for a particular railway track. For this model case, we have found out the ratio of the open-circuit and short-circuit impedance measured at the input of the track circuit Eq. (10).

2. Determining Open-Circuit Impedance

As stated in the introduction, the DITO settings for modified traffic conditions are corrected (re-calibrated) at predetermined intervals based on the measurements. The calibration is performed when the section is not occupied. The question is, how long the distance of the section of railway line from the source can be measured to obtain the input impedance of an open circuit using alternating current with a frequency of 75 Hz or 275 Hz. Thus, at what shortest distance l_0 the input impedance changes minimal (with a required tolerance), for example, when the rail circuit is powered by a 5A current source. The power supply is carried out at the measuring point between the two rails of the same track as shown in Fig. 1.

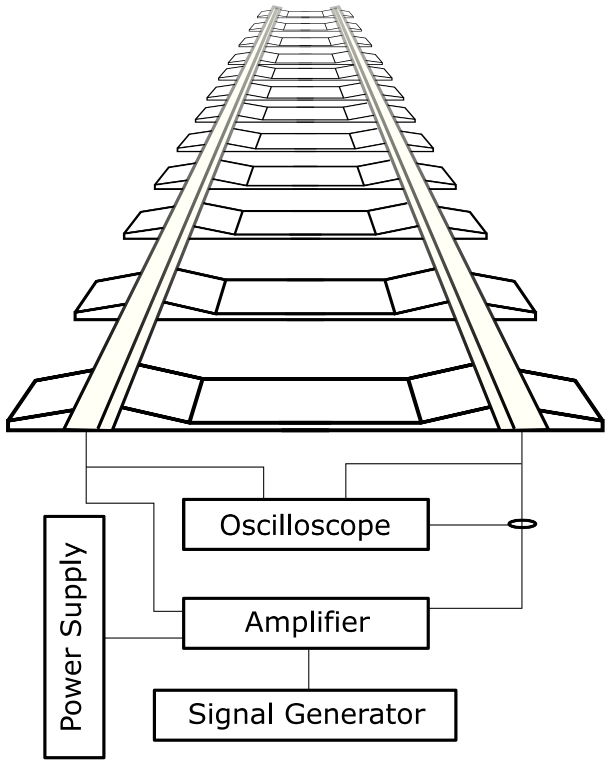

Fig. 1: Block diagram for measuring traction parameters.

The two-port networks are the passive and longitudinally symmetrical ones. Thus, in the case of the railway traction, the image parameters of uniformly distributed line can be used to calculate the input impedance. The open-circuit impedance is calculated from the input voltage and current ratios Eq. (4), Eq. (5) and Eq. (6).

$$\underline{U}_{10} = \underline{U}_{20} \cosh(\underline{\gamma} x), \tag{4}$$

$$\underline{I}_{10} = \frac{\underline{U}_{20}}{\underline{Z}_v} \sinh(\underline{\gamma} x) = \\ = \frac{\frac{\underline{U}_{10}}{\cosh(\underline{\gamma} x)}}{\underline{Z}_v} \sinh(\underline{\gamma} x) = \frac{\underline{U}_{10}}{\underline{Z}_v} \tanh(\underline{\gamma} x), \tag{5}$$

$$\underline{Z}_0 = \frac{\underline{Z}_v}{\tanh(\underline{\gamma} x)}, \tag{6}$$

where:

- $\underline{U}_{10}$ is the open-circuit voltage at the input at the point of measurement, i.e., at the beginning of the test section,
- $\underline{U}_{20}$ is the voltage at the end of the unoccupied section (at a distance of $x = l_0$),
- $\underline{Z}_v$ is the image (characteristic) impedance $\underline{Z}_v = \sqrt{\frac{\underline{Z}}{\underline{Y}}}$,
- $\underline{\gamma}$ is the propagation constant $\underline{\gamma} = \underline{Z} \cdot \underline{Y}$,
- x is the distance from the measuring point (the beginning of the section).

First of all, we are interested in the constant open-circuit impedance value $\underline{Z}_0$ for $x = l_0$, where l_0 is the limiting (critical) length of the segment. At distance l_0 the open-circuit impedance at the input is no longer changing with an increasing x-coordinate. The open-circuit impedance values $\underline{Z}_0$ are then crucial for determining the ratio $\underline{F}(x)$. From the calculated waveform of the open-circuit impedance module values $\underline{Z}_0$ are visible in Fig. 2 up to 600 m in length and in Fig. 3 up to 3000 m (for 75 Hz). It is clear that if the measured section is longer than 2500 m, we can expect a constant (steady) input impedance value of the unoccupied section (open circuit).

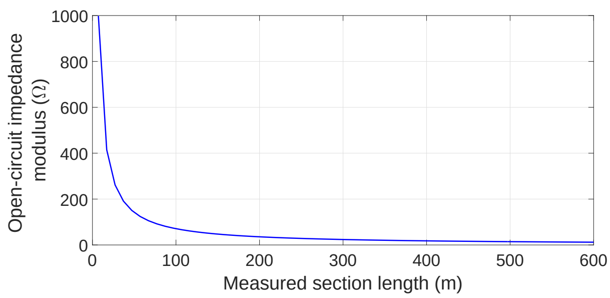

Fig. 2: Dependency of the unoccupied module $\underline{Z}_0$ on the length of the measured section.

The impedance module sharply decreases - see Fig. 2. It settles at the value 4. For small values of x, the graph is drawn with a high input value of the open-circuit impedance module. The situation is more clearly seen from the graph for the distances from 500 m to 3000 m, see Fig. 3. Figure 4 shows more complicated dependence of the phase input impedance of the unoccupied section.

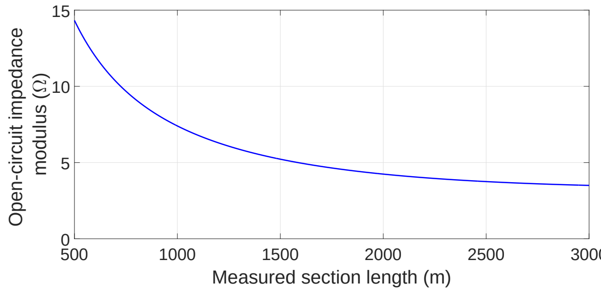

Fig. 3: Detail of the module $\underline{Z}_0$ for distance from 500 m.

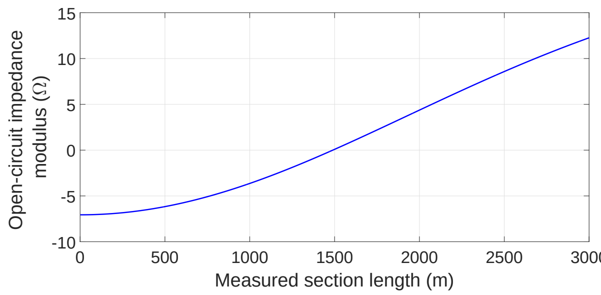

Fig. 4: Dependence of the $\underline{Z}_0$ phase of the unoccupied section on the length of the measured section.

The shape of the curve shows a capacitive character at first, which is logical for short parallel conductors with a low transverse conductivity. At about 1500 m, the circuit is in resonance, and the character of the circuit is further changed to inductive. The inductive nature of the current loops, which are closed over the transverse conduction between the rails, is already clearly applied here.

The DITO device will "calibrate" the new parameters at intervals when the section is unoccupied. Thus, a constant open-circuit impedance value is considered when calculating the ratio $\underline{F}(x)$. This impedance value is measured when the instrument is calibrated. When the length of the measured section increases, it does not change much. In the example modeled here we chose $\underline{Z}_0 = (3.42 + 0.74j)\ \Omega$ (designated for 3000 m).

3. Determining the Impedance of the Occupied Circuit

In the case of the presence of a traction vehicle in the measured section, the rails of the occupied tracks are shunt (are replaced by short-circuiting). The input impedance of the measured section decreases with the vehicle approaching to the measuring point. The short-circuit input impedance is again calculated from the ratio of short-circuit voltage to the short-circuit current Eq. (7), Eq. (8) and Eq. (9).

$$\begin{aligned} \underline{U}_{1S} &= \underline{Z}_v \underline{I}'_{2S} \sinh(\underline{\gamma} x) = \\ &= \underline{Z}_v \frac{\underline{I}_{1S}}{\cosh(\underline{\gamma} x)} \sinh(\underline{\gamma} x) = \\ &= \underline{Z}_v \underline{I}_{1S} \tanh(\underline{\gamma} x), \end{aligned} \tag{7}$$

$$\underline{I}_{1S} = \underline{I}'_{2S} \cosh(\underline{\gamma} x), \tag{8}$$

$$\underline{Z}_S = \underline{Z}_v \tanh(\underline{\gamma} x), \tag{9}$$

where:

- $\underline{I}_{1S}$ is the input short-circuit current at the measuring point, i.e., at the beginning of the test section under investigation,
- $\underline{I}'_{2S}$ is the current in the place of the short-circuit.

The graphical dependencies of the short-circuit impedance $\underline{Z}_S$ on the vehicle's distance from the measured point (from the beginning of the section) are, at 75 Hz, shown in Fig. 5 for the module and Fig. 6 for the phase.

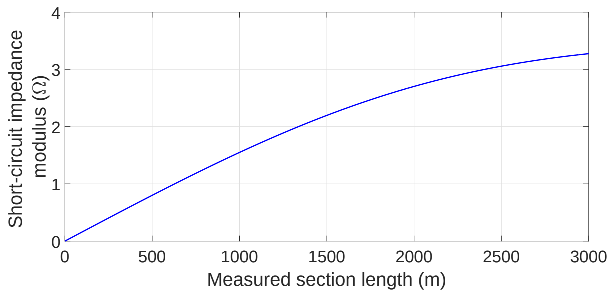

Fig. 5: Dependence of the $\underline{Z}_S$ module on the vehicle's distance from the measuring point.

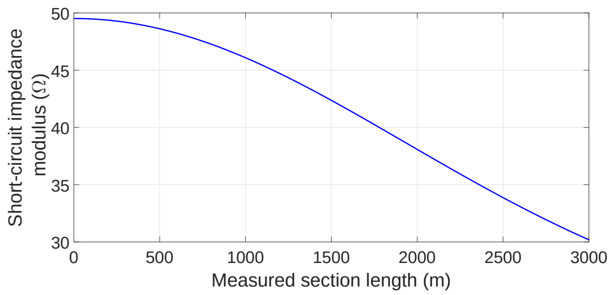

Fig. 6: Dependence of the $\underline{Z}_S$ phase on the vehicle's distance from the measuring point.

4. Calculate the Ratio $\underline{\mathbf{F}}(\mathbf{x})$

Ratio $\underline{F}(x)$ expresses the proportion of constant open-circuit input impedance (it will be measured on an unoccupied track at defined intervals, always for the same length of the segment) to the variable short-circuit impedance Eq. (10). The graphical representation of ratio $\underline{F}(x)$ is shown in Fig. 5 (for the module) and Fig. 6 (for the phase).

$$\underline{F}(x) = \frac{\underline{Z}_S(x)}{\underline{Z}_0(l_k)} = \frac{1}{\tanh(\underline{\gamma}x)\tanh(\underline{\gamma}lk)}. \tag{10}$$

The tanh value for the positive argument ranges from 0 to 1. It can be said that when the argument of ratio $\underline{F}(x)$ is equal to 2.5 the tanh value is very close to 1, with the argument, equal to 0. It needs not being considered in this case. Therefore, the lower limit of this ratio may theoretically be 1, but practically it is greater.

The relationship can also be adjusted to Eq. (11):

$$\begin{aligned}\underline{F}(x) &= \frac{1}{\tanh(\underline{\gamma}x)\tanh(\underline{\gamma}lk)} = \\ &= \frac{\cosh(\underline{\gamma}(l_k+x)) + \cosh(\underline{\gamma}(l_k-x))}{\cosh(\underline{\gamma}(l_k+x)) - \cosh(\underline{\gamma}(l_k-x))}.\end{aligned} \tag{11}$$

The module values $\underline{F}(x)$ in relation to the short-circuit distance are shown in Fig. 5 and Fig. 7 and the ratio phase values $\underline{F}(x)$ in Fig. 8.

Based on the automatic measurement of the open-circuit impedance at regular intervals on an unoccupied track, parameters R, L, C, G are recalculated and the instrument calibrated for changed conditions, e.g. weather.

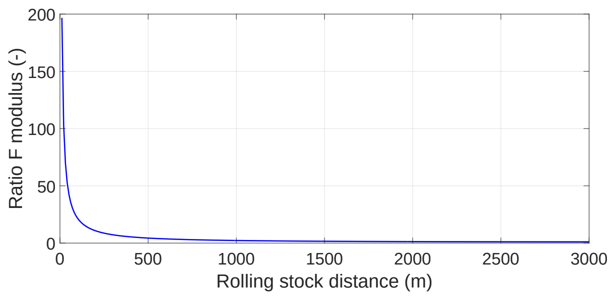

Fig. 7: Dependence of the module ratio $\underline{F}(x)$ on distance x of the vehicle from the measuring point.

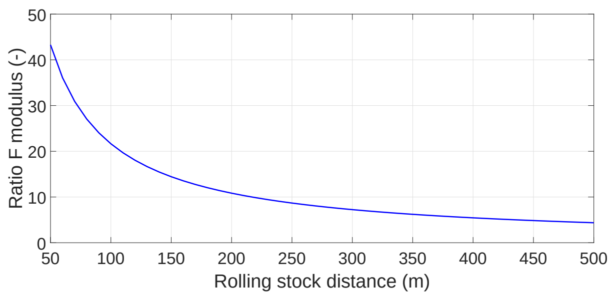

Fig. 8: Module ratio $\underline{F}(x)$ - detail from 50 m to 500 m.

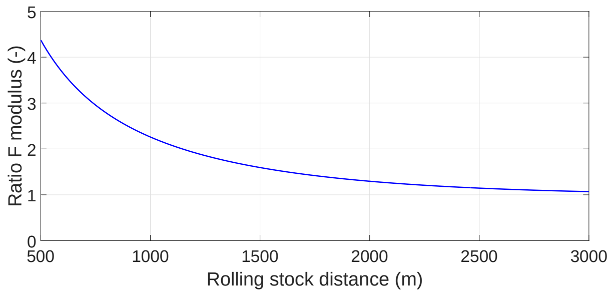

Fig. 9: Module ratio $\underline{F}(x)$ - detail from 500 m to 3000 m.

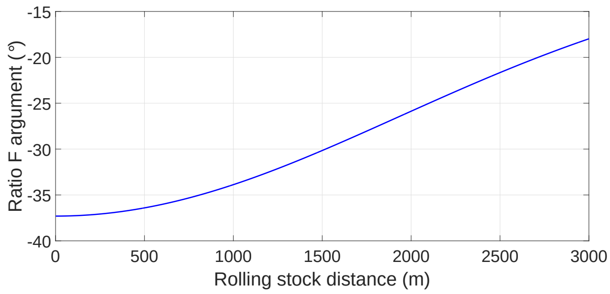

Fig. 10: Dependence of the phase ratio $\underline{F}(x)$ on the vehicle's distance from the measured site.

The ratio of module $\underline{F}(x)$ at the selected reference value $\underline{Z}_0 = (3.42+0.74j)\ \Omega$ reaches a value of about 10 in about 218 m. This ratio, at first glance, decreases by 1.595 at 1.5 km, 1.34 at 1.9 km, 1.013 at 4.66 km, but then again slightly increases from 29.7 km. It stabilizes at value 1.034. The limit distance l_1 at which the DITO device is still able to register the short-circuiting of the rails on the basis of the module's values $\underline{F}(x)$ occurs at the ratio $F(x) > 1.3$ (at 75 Hz). In this model example this value is achieved in distance $l_1 = 2000\ m$. At a greater distance where the ratio $\underline{F}(x)$ and the input impedance do not change during the short-circuit. Thus, ratio $F(x) < 1.3$ cannot be used for the speed estimate and for the track occupancy indication. In this case, it is possible to use the relatively significant change in the phase of the ratio $\underline{F}(x)$.

5. Conclusion

Ensuring the safety of train crossings is currently an increasingly difficult challenge. Early closure of a crossing through signaling or gates also brings security risks from undisciplined drivers and often disproportionately hinders transport. The optimum time-to-lock setting by signaling or barrier requires a reliable positioning and speed system of the train approaching the crossing. One of the principles that can be used to locate the train and determine its speed is to measure the waveform of the impedance of the track circuit short-circuited by the approaching train.

In order to prepare the design of the equipment for this activity, we prepared a methodology for analyzing the changes in the impedances ratios of the occupied and unoccupied section. From these backgrounds, designers of the occupancy indication section judge how to set the input of this device so that it can function properly. The results of this paper may be helpful in doing so.

Acknowledgment

This publication is supported by project SP2017/152 "Research of antenna systems, diagnostics and reliability of electrical machines and equipment" and by project TA04031780.

References

[1] SANTOS, J., M. HEMPEL and H. SHARIF. Sensing Techniques and Detection Methods for Train Approach Detection. In: *IEEE Vehicular Technology Conference (VTC-Fall)*. Las Vegas: IEEE, 2013, pp. 1–5. ISBN 978-1-4673-6187-3. DOI: 10.1109/VTCFall.2013.6692407.

[2] TURNER, S. A track sensor for predicting train arrival time. In: *Innovations Deserving Exploratory Analysis Programs* [online]. 2009. Available at: `http://onlinepubs.trb.org/onlinepubs/IDEA/FinalReports/HighSpeedRail/HSR-50Final_Report.pdf`.

[3] IVANEK L., V. MOSTYN, K. SCHEE and J. GRUN. The Sensitivity of the Input Impedance Parameters of Track Circuits to Changes in the Parameters of the Track. *Advances in Electrical and Electronic Engineering*. 2017, vol. 15, no. 1, pp. 77–83. ISSN 1336-1376. DOI: 10.15598/aeee.v15i1.1996.

[4] COLAK, K. and M. H. HOCAOGLU. Calculation of rail potentials in a DC electrified railway system. In: *38th International Universities Power Engineering Conference*. Thessaloniki: IEEE, 2003, pp. 1–8.

[5] SZELAG, A. Rail track as a lossy transmission line Part I: Parameters and new measurement methods. *Archives of Electrical Engineering*. 2000, vol. 49, no. 3–4, pp. 407–423. ISSN 1427-4221.

[6] SZELAG, A. Rail track as a lossy transmission line. Part II: New method of measurements simulation and in situ measurements. *Archives of Electrical Engineering*. 2000, vol. 49, no. 3–4, pp. 425–453. ISSN 1427-4221.

[7] HILL, R. J. and D. C. CARPENTER. Rail track distributed transmission line impedance and admittance: theoretical modeling and experimental results. *IEEE Transaction Vehicular Technology*. 1993, vol. 42, no. 2, pp. 225–241. ISSN 1427-4221. DOI: 10.1109/25.211460.

[8] HILL, R. J., D. C. CARPENTER and T. TASAR. Railway track admittance, earth-leakage effects and track circuit operation. In: *Technical Papers Presented at the 1989 IEEE/ASME Joint Railroad Conference*. Philadelphia: IEEE, 1989, pp. 55–62. ISBN 999-2-9844-14. DOI: 10.1109/RRCON.1989.77281.

[9] HOLMSTROM, F. R. The model of conductive interference in rapid transit signaling systems. *IEEE Transactions on Industry Applications*. 1986, vol. IA-22, no. 4, pp. 756–762. ISSN 0093-9994. DOI: 10.1109/TIA.1986.4504788.

[10] KOLAR, V., A. NEUMANN, R. HRBAC and T. MLCAK. Simulation and Measurement of Selected Electrical Parameters for Electric Drainage. In: *ELEKTRO 11th International Conference*. Strbske Pleso: IEEE, 2016, pp. 320–324. ISBN 978-1-4673-8698-2. DOI: 10.1109/ELEKTRO.2016.7512089.

About Authors

Lubomir IVANEK was born in Frydek Mistek in the Czech Republic. He graduated from the VSB–Technical University Ostrava, Faculty of Mechanical and Electrical Engineering, earned his Ph.D. degree from the Czech Technical University in Prague, Department of Theoretical Electrical Engineering. Associate Professor degree received at the VSB–Technical University of Ostrava in the field of Theoretical Electrical Engineering. His research involves the waves propagation and antennas, mathematical modelling of the electromagnetic field, stray current under electric tractions.

Petr ORSAG was born in Prerov, the Czech Republic in 1963. He received his M.Sc. degree in Electrical Machines and Electrical Drives from VSB–Technical University of Ostrava in 1988 and Ph.D. degree from VSB–Technical University of Ostrava in 1999. At present he is a senior lecturer at VSB–Technical University of Ostrava. His field of interest is electromechanical systems diagnostics, power efficiency of the adjustable speed drives and modelling of electrical systems.

Vladimir MOSTYN was born in Prilepy in the Czech Republic. He received the M.Sc. degree in Electrical Engineering in 1979 from the VSB–Technical University of Ostrava, Czech Republic. Since 1990, he has been an Assistant Professor with the Department of Robotics and he received the Ph.D. degree in 1996 in Control Engineering at the same university. In 2006 he was appointed by the president of Slovak Republic to degree Professor in branch Production Systems with Industrial Robots and Manipulators after a successful accomplishment of the process of awarding a professorship at the Technical University of Kosice, Slovak Republic. Now he is working as professor at the Department of Robotics at the Faculty of Mechanical Engineering at the VSB–Technical University of Ostrava, Czech Republic. He is the author of two books and more than 80 articles. His research interests include robotics, simulation of the complex mechatronic systems and computer aided systems. Profesor Vladimir Mostyn is an Associate Editor of the journal MM Science Journal and the member of Czech Association of Robotic Surgery.

Karel SCHEE was born in Opava in the Czech Republic. He received his M.Sc. from VSB–TUO in 1999. His research interests include automation of rail transport.